

A variational approach to Bogoliubov excitations and dynamics of dipolar Bose-Einstein condensates

Manuel Kreibich, Jörg Main and Günter Wunner

1. Institut für Theoretische Physik, Universität Stuttgart, 70550 Stuttgart, Germany

Abstract. We investigate the stability properties and the dynamics of Bose-Einstein condensates with axial symmetry, especially with dipolar long-range interaction, using both simulations on grids and variational calculations. We present an extended variational ansatz which is applicable for axial symmetry and show that this ansatz can reproduce the lowest eigenfrequencies of the Bogoliubov spectrum, and also the corresponding eigenfunctions. Our variational ansatz is capable of describing the roton instability of pancake-shaped dipolar condensates for arbitrary angular momenta. After investigating the linear regime we apply the ansatz to determine the dynamics and show how the angular collapse is correctly described within the variational framework.

PACS numbers: 03.75.Kk, 67.85.De, 05.45.-a

1. Introduction

As an alternative to the direct numerical solution of the Gross-Pitaevskii equation (GPE) and the Bogoliubov-de Gennes equations (BDGE), which describe the ground states and excitations of Bose-Einstein condensates (BECs) [1], Rau *et al* [2, 3] proposed a variational approach with coupled Gaussians to calculate stationary solutions and the stability of a condensate using the methods of nonlinear dynamics. Specifically, they used the time-dependent variational principle (TDVP) to map the GPE to a nonlinear dynamical system for the variational parameters whose fixed points correspond to ground states of the GPE. The stability can be analysed by means of the linearised equations of motion, i. e. in terms of the eigenvalues of the Jacobian. However, it remained unclear whether there is a direct relationship between the eigenvalues of the BDGE and those of the Jacobian. In a recent work [4] we analysed this problem for spherically symmetric systems and showed that a variational ansatz with coupled Gaussians has limitations in that it can only describe excitations with an angular momentum $l \leq 2$. We present an extended variational ansatz and show that there is indeed a good agreement between the lowest eigenvalues of the BDGE and the Jacobian for arbitrary angular momenta, with or without additional long-range interaction (LRI).

A variational ansatz with a single Gaussian [5] cannot reproduce the biconcave structure of dipolar condensates revealed in certain parameter regions [6, 7]. Using

the variational ansatz of coupled Gaussians, however, it was possible to obtain non-Gaussian shapes [2,3,8] and to reproduce the wave function and the energy of structured ground states. Additionally, the stability was analysed which revealed that the collapse breaks the axial symmetry within the variational approach. However, the ansatz used in Ref. [8] is only capable of describing modes with angular momentum $m = 0$ and $m = 2$ (see discussion in [4]). The angular collapse with $m = 3$ symmetry, calculated numerically on a grid in [9], is therefore not accessible to this variational ansatz of coupled Gaussians.

Several extensions of the Gaussian ansatz have been proposed in the literature [10–12], but they allow for no systematic inclusion of arbitrary angular momenta. It is the purpose of this work to extend the variational ansatz of coupled Gaussians in such a way that an instability with an arbitrary projection of the angular momentum on the z axis can be described for systems with axial symmetry. We present an extended variational ansatz including angular exponentials $\exp(im\phi)$, which are eigenfunctions of the z component of the angular momentum operator. This enables us to describe modes with arbitrary angular momentum within the variational framework, which will be demonstrated by applying the ansatz to condensates with contact interaction only, and with dipole-dipole interaction (DDI).

In Sec. 2 we discuss the stability and excitations of BECs. We first present the method of numerically solving the BDGE, which we need for a comparison with the variational method. The extended variational ansatz is described and applied to calculate the eigenfrequencies of elementary excitations. We compare the results with those obtained from the full-numerical solution. In Sec. 3 we apply the variational ansatz to calculate the time evolution of a dipolar BEC and demonstrate that the ansatz can describe the angular collapse. In Sec. 4 we draw conclusions and give an outlook on future work.

2. Stability and excitations

The time-dependence of a BEC is described in the mean-field approximation by the time-dependent GPE [1]

$$i\hbar \frac{\partial \psi}{\partial t}(\mathbf{r}, t) = \left[-\frac{\hbar^2}{2M} \Delta + \frac{M}{2} \omega_\rho^2 (\rho^2 + \lambda^2 z^2) + N \Phi_{\text{int}}(\mathbf{r}, t) \right] \psi(\mathbf{r}, t), \quad (1)$$

where N is the particle number,

$$\Phi_{\text{int}}(\mathbf{r}, t) = \int d^3 r' V_{\text{int}}(\mathbf{r} - \mathbf{r}') |\psi(\mathbf{r}', t)|^2 \quad (2)$$

the mean field produced by the inter-particle interaction, $\psi(\mathbf{r}, t)$ the wave function of the condensate normalised to unity, and M the mass of the atom species. The harmonic external trap is given by the trapping frequencies ω_ρ and ω_z in the ρ and z direction, and can be characterised by the trap aspect ratio $\lambda = \omega_z/\omega_\rho$. We measure all lengths

in units of the harmonic oscillator length $a_{\text{ho}} \equiv \sqrt{\hbar/M\omega_\rho}$, all frequencies in units of ω_ρ , and the time in units of $1/\omega_\rho$. A stationary solution of Eq. (1) has the time dependence $\psi(\mathbf{r}, t) = \psi(\mathbf{r}) \exp(-i\mu t/\hbar)$, where μ is the chemical potential of the condensate.

The interaction potential is given by [13]

$$V_{\text{int}}(\mathbf{r} - \mathbf{r}') = \frac{4\pi a \hbar^2}{M} \delta(\mathbf{r} - \mathbf{r}') + \frac{\mu_0 \mu_{\text{m}}^2}{4\pi} \frac{1 - 3\frac{(z-z')^2}{(\mathbf{r}-\mathbf{r}')^2}}{|\mathbf{r} - \mathbf{r}'|^3}. \quad (3)$$

The quantity a is the s-wave scattering length and μ_{m} the magnetic moment of the atom species and is, e. g., $\mu_{\text{m}} = 6\mu_{\text{B}}$ (μ_{B} the Bohr magneton) for ^{52}Cr [14]. The dipoles are assumed to be aligned along the z axis by an external magnetic field. The interactions can be characterised by the dimensionless parameters Na/a_{ho} and $D \equiv N \frac{\mu_0}{4\pi} \frac{M}{\hbar^2} \frac{\mu_{\text{m}}^2}{a_{\text{ho}}}$ [15]. In this article, we investigate BECs with and without LRI. For the condensate with DDI we use values of $D = 30$ and $\lambda = 7$, since for these parameters structured ground states appear [3,6]. For the BEC without LRI we use a trap aspect ratio of $\lambda = \sqrt{8}$, which was used in experiments [16]. The scattering length can be tuned in a wide range via Feshbach resonances [17]. Thus, we use this quantity as a free parameter in our calculations.

2.1. Full-numerical treatment

Besides the variational approach we also perform grid calculations to directly solve the GPE and BDGE, which allows us to compare both methods. Before solving the BDGE, one first needs to find the ground state of a BEC. In this work, we use the imaginary time evolution (ITE) for this task. We evolve an initial wave function on a grid in imaginary time τ defined by $\tau \equiv it$, and as time evolves the wave function converges to the ground state. The time evolution on the grid is done via the split operator method [18], in which the time evolution operator in imaginary time is given by

$$e^{-\hat{H}\Delta\tau/\hbar} = e^{-\frac{1}{2}\hat{T}\Delta\tau/\hbar} e^{-\hat{V}\Delta\tau/\hbar} e^{-\frac{1}{2}\hat{T}\Delta\tau/\hbar} + \mathcal{O}(\Delta\tau^3), \quad (4)$$

where \hat{T} and \hat{V} represent the kinetic and the potential terms of the mean-field Hamiltonian, respectively. The action of the kinetic part is trivial in Fourier space, whereas the action of the potential part is trivial in real space. Since we are dealing with a cylindrically symmetric system, we can use the Fourier-Hankel algorithm of [15] to compute the necessary Fourier transforms for a time step and the dipolar integrals via the convolution theorem.

To derive the BDGE, one starts from the usual ansatz for the perturbation of a stationary state ψ_0 with chemical potential μ [1]

$$\psi(\mathbf{r}, t) = [\psi_0(\mathbf{r}) + \lambda (u(\mathbf{r}) e^{-i\omega t} + v^*(\mathbf{r}) e^{i\omega^* t})] e^{-i\mu t/\hbar}, \quad (5)$$

where ω is the frequency and λ the amplitude of the perturbation ($|\lambda| \ll 1$). After inserting this ansatz into the time-dependent GPE (1), while neglecting terms of

second order in λ , and collecting terms evolving in time with $\exp(-i\omega t)$ and $\exp(i\omega t)$, respectively, one obtains the BDGE

$$\begin{aligned} \hbar\omega u(\mathbf{r}) = & \left[H_0 - \mu + \int d^3r' V_{\text{int}}(\mathbf{r} - \mathbf{r}') |\psi_0(\mathbf{r}')|^2 \right] u(\mathbf{r}) \\ & + \int d^3r' V_{\text{int}}(\mathbf{r} - \mathbf{r}') \psi_0^*(\mathbf{r}') u(\mathbf{r}') \psi_0(\mathbf{r}) \\ & + \int d^3r' V_{\text{int}}(\mathbf{r} - \mathbf{r}') \psi_0(\mathbf{r}') v(\mathbf{r}') \psi_0(\mathbf{r}), \end{aligned} \quad (6a)$$

$$\begin{aligned} -\hbar\omega v(\mathbf{r}) = & \left[H_0 - \mu + \int d^3r' V_{\text{int}}(\mathbf{r} - \mathbf{r}') |\psi_0(\mathbf{r}')|^2 \right] v(\mathbf{r}) \\ & + \int d^3r' V_{\text{int}}(\mathbf{r} - \mathbf{r}') \psi_0^*(\mathbf{r}') u(\mathbf{r}') \psi_0^*(\mathbf{r}) \\ & + \int d^3r' V_{\text{int}}(\mathbf{r} - \mathbf{r}') \psi_0(\mathbf{r}') v(\mathbf{r}') \psi_0^*(\mathbf{r}), \end{aligned} \quad (6b)$$

where $H_0 = -\frac{\hbar^2}{2M}\Delta + \frac{M}{2}\omega_\rho^2(\rho^2 + \lambda^2 z^2)$. Due to the cylindrical symmetry, we can make an ansatz for the solutions

$$u(\mathbf{r}) = e^{im\phi} u(\rho, z), \quad v(\mathbf{r}) = e^{im\phi} v(\rho, z), \quad (7)$$

where m is the usual quantum number of the projection of the angular momentum operator on the z axis. Since the Laplacian in cylindrical coordinates applied to the ansatz (7) yields

$$\Delta e^{im\phi} u(\rho, z) = \left(\Delta_{\rho,z} - \frac{m^2}{\rho^2} \right) e^{im\phi} u(\rho, z), \quad (8)$$

which only depends on $|m|$, there is a degeneracy of the eigenmodes for $|m| > 0$. Thus, we can restrict ourselves to solutions with $m \geq 0$. Another symmetry of the system is the reflection at the $z = 0$ plane ($z \rightarrow -z$). Therefore, the solutions can be described by the parity $\pi_z = \pm 1$ under this reflection. We denote the set of quantum numbers with m^{π_z} . There are always solutions of the BDGE for $\omega = 0$ and the trapping frequencies, which represent the gauge mode and the centre of mass oscillations [1, 4].

We solve the linear, nonlocal BDGE (6) by calculating the matrix elements of the right-hand side in coordinate representation by means of the Fourier-Hankel algorithm [15]. The lowest eigenvalues of the resulting high-dimensional matrix are then calculated using the Arnoldi iteration [19], implemented in the Fortran ARPACK routines [20].

The solutions of the BDGE (6) yield the frequencies and the shape of elementary oscillations of the condensates. But it may happen that the Bogoliubov spectrum of the ground state of a dipolar BEC contains imaginary frequencies [9], which correspond to dynamical instabilities. A small perturbation of the ground state then leads to an exponential decay.

We calculated the ground states and Bogoliubov spectra for a BEC with an attractive short-range interaction (SRI) only ($D = 0$) and a trap aspect ration of

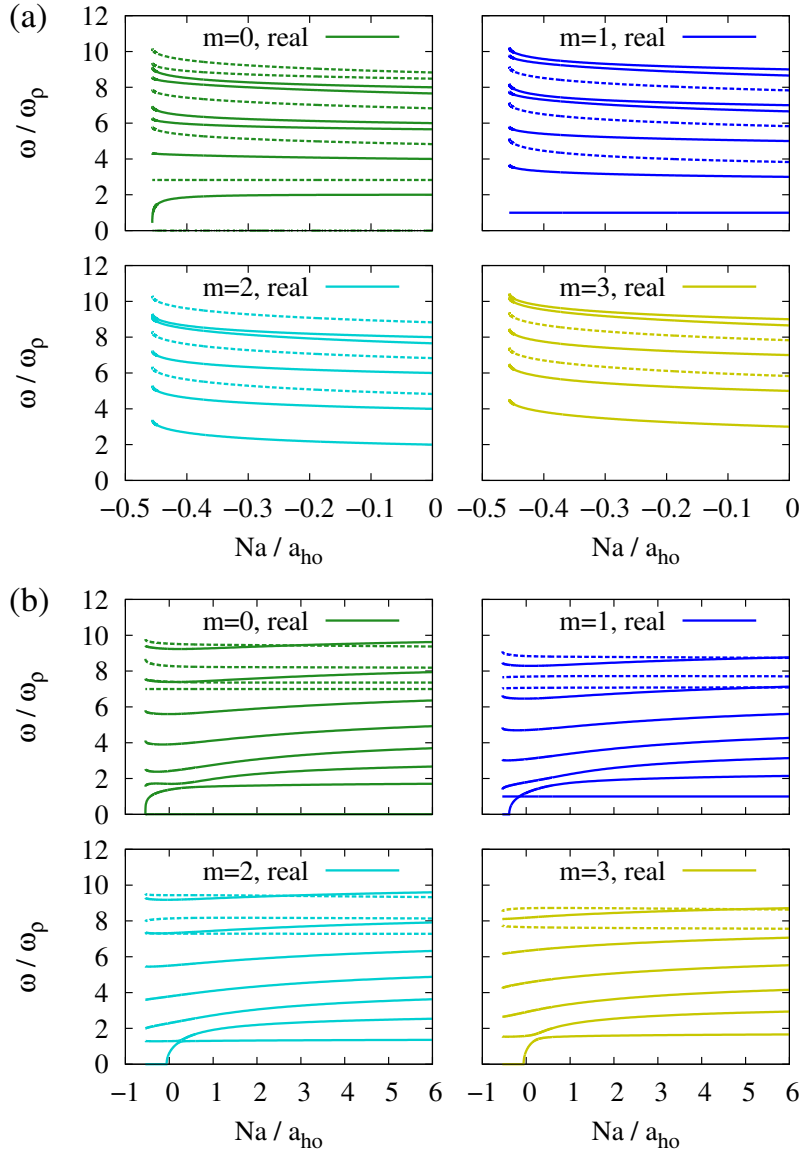


Figure 1. Bogoliubov spectra of the ground states for (a) a BEC with short-range interaction ($\lambda = \sqrt{8}, D = 0$) and (b) a dipolar BEC ($\lambda = 7, D = 30$) as a function of the scattering length Na/a_{ho} (shown are the real parts of the frequencies) with even (solid) and odd (dashed) modes. Both spectra feature the lowest $m = 0$ mode, whose frequency goes to zero when the scattering length reaches the critical value a_{crit} , and the centre of mass oscillations at the trapping frequencies. Unique for the dipolar BEC are the lowest excitations for higher angular momenta $m > 0$, which turn unstable and mark a local collapse of the condensate.

$\lambda = \sqrt{8}$, and for a dipolar BEC with $\lambda = 7$ and $D = 30$, for which it was shown that the structured ground state changes its stability in a pitchfork bifurcation [8] at the scattering length $Na/a_{\text{ho}} \approx -0.215$ ‡. The structured ground states, where the

‡ In [8] a Gaussian ansatz with $N_G = 5$ Gaussians was used. The scattering length, where the bifurcation takes place, however, converges slowly with increasing number of Gaussians and may be different in our calculations.

maximum of particle density lies away from the centre, appear in isolated regions in parameter space with $\lambda = 7, 11, 15, \dots$ [6]. For our choice of parameters, $\lambda = 7$ and $D = 30$, the ground state assumes a biconcave structure for the scattering lengths $-0.546 \lesssim Na/a_{\text{ho}} \lesssim 1.4$.

For both systems ground states only exist for scattering lengths larger than the critical scattering length, $a \geq a_{\text{crit}}$. For the condensate with SRI, the critical scattering length is given by $Na_{\text{crit}}/a_{\text{ho}} \approx -0.457$. BECs at small negative scattering lengths may exist, since the kinetic energy compensates the attractive interaction and stabilises the condensate. The critical scattering length was probed experimentally in a condensate of ^{85}Rb , and significant deviations from the results of the GPE were measured [21], which may be explained by taking into account higher-order nonlinear effects [22]. The critical scattering length of a dipolar BEC considerably depends on the trap geometry, in our case ($\lambda = 7$, $D = 30$) its value is given by $Na_{\text{crit}}/a_{\text{ho}} \approx -0.546$. A good agreement between experiment and the results of the GPE was found [23].

Fig. 1 shows the Bogoliubov spectra. Since both systems have already been considered in the literature (see, e. g., [24] for the BEC with SRI, and [15] for the dipolar BEC), we only give a short review. The spectrum of the BEC without LRI (Fig. 1a) can be understood by taking the limit $a \rightarrow 0$, which yields the exact eigenvalues of the cylindrically symmetric harmonic oscillator

$$\frac{\omega_{n_\rho, n_z, m}}{\omega_\rho} = 2n_\rho + |m| + \lambda n_z, \quad (9)$$

where $n_{\rho, z} \in \mathbb{N}_0$ are the quantum numbers for excitations along the ρ and z direction, respectively. When decreasing the scattering length towards the critical value, below which no stationary solutions exist anymore, the frequencies vary slightly, which means that in this regime the dynamics is dominated by the external trap, and the interaction acts as a quasi perturbation. Just slightly above the critical point the lowest mode with $m = 0$ drops to zero, which marks the global collapse of the condensate. The oscillations of the centre of mass, which constantly lie at the trapping frequencies, are represented by the lowest odd $m = 0$ mode ($\omega/\omega_\rho = \sqrt{8}$) and the lowest even $m = 1$ mode ($\omega/\omega_\rho = 1$).

The Bogoliubov spectrum of the dipolar condensate (Fig. 1b) indicates a stable condensate when the scattering length is far from the critical point. However, for decreasing scattering length, not only the mode with $m = 0$ but also frequencies for higher angular momenta decrease and drop to zero. At these points, those modes become unstable, as the eigenfrequencies are imaginary. Fig. 2 shows the real and imaginary parts of the lowest eigenfrequencies for the angular momenta $m = 1, \dots, 5$. The modes with $m = 2$ and $m = 3$ are the first ones which turn unstable, and thus mark the local collapse of the condensate. This means, that collapse occurs via local density-fluctuations in contrast to a global collapse, where the condensate collapse to the trap centre [9]. In Sec. 3 we discuss the dynamics of such a local collapse, with the result that an extended variational ansatz is necessary to describe the collapse. This is

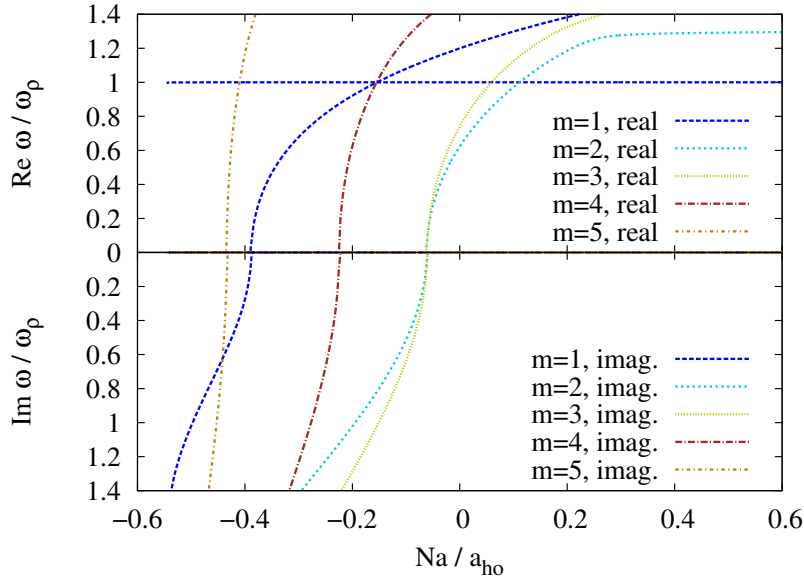


Figure 2. The lowest modes of the Bogoliubov spectrum of the dipolar BEC from Fig. 1b. Shown are the real and also imaginary parts of the frequencies. In our resolution of the scattering length, the modes with $m = 2$ and $m = 3$ turn unstable simultaneously, but the latter has a higher imaginary frequency below the critical scattering length, which means that this mode dominates the collapse in the vicinity of the stationary solution.

a unique feature of dipolar BECs and is related to the biconcave structure of the ground state occurring for specific trapping geometries [8, 9]. These instabilities are referred to as rotons, or, more specifically, as discrete “angular rotons”, since these excitations assume a shape with azimuthal nodal surfaces [6].

Worth mentioning also is the avoided crossing in the lowest modes for the angular momenta $m = 0, 2, 3$, whereas for $m = 1$ there is a regular crossing since $\omega = \omega_\rho$ is an exact solution for every scattering length, which does not allow for an avoided crossing.

2.2. Variational approach

The grid calculations are very accurate, if grid size and resolution are chosen carefully, but computationally expensive. The variational method provides an alternative in that the computation time reduces significantly compared to grid calculations. With this motivation, Rau *et al* [2, 3, 8] used the variational ansatz

$$\psi = \sum_{k=1}^{N_G} e^{i(A_x^k x^2 + A_y^k y^2 + A_z^k z^2 + \gamma^k)} \quad (10)$$

to calculate stationary solutions and excitations of dipolar condensates. Here, N_G is the number of Gaussians, A_x^k , A_y^k and A_z^k describe the widths and γ^k the amplitude of each Gaussian. The quantities $(A_x^k, A_y^k, A_z^k, \gamma^k)$ are the variational parameters of this ansatz. In a recent article [4] we showed that the variational ansatz with coupled

Gaussians can only describe modes with an angular momentum of $l \leq 2$, $|m| \leq 2$. For that reason we proposed an extended variational ansatz with coupled Gaussians and spherical harmonics, which can describe modes with arbitrary angular momenta in spherically symmetric systems. We found a good agreement of the lowest eigenmodes with those obtained by grid calculations.

For the systems with axial symmetry considered here, this ansatz is not applicable, since the angular momentum is no longer a good quantum number and therefore the angular part of the excitations is not described by spherical harmonics. However, the z component of the angular momentum, represented by the quantum number m and the eigenfunctions $\exp(im\phi)$, is still conserved. Using this knowledge we construct an extended variational ansatz, which is specific to cylindrically symmetric systems, and which is given by

$$\psi = \sum_{k=1}^{N_G} \left(1 + \sum_{m \neq 0} \sum_{p=0,1} d_{m,p}^k \rho^{|m|} z^p e^{im\phi} \right) e^{-A_\rho^k \rho^2 - A_z^k z^2 - p_z^k z - \gamma^k}. \quad (11)$$

The complex variational parameters A_ρ^k and A_z^k describe the width in the ρ and z direction, p_z^k is the displacement along the z axis, and γ^k describes the amplitude of each Gaussian. With these parameters alone, the wave function does not depend on the angular coordinate ϕ , thus the parameters $(A_\rho^k, A_z^k, p_z^k, \gamma^k)$ are responsible only for any $m = 0$ excitation. To account for higher angular momenta and arbitrary parity π_z , we include the sums over m and p in the brackets ($\pi_z = +1$ belongs to $p = 0$, and $\pi_z = -1$ to $p = 1$). The amplitude of each of these excitations is given by the variational parameters $d_{m,p}^k$.

To derive the equations of motion for the variational parameters, we follow the procedure in [2,4] and apply the Dirac-Frankel-McLachlan TDVP [25,26]. It states that the norm of the difference between the left- and the right-hand side of the Schrödinger or GPE

$$I = \|\dot{i}\chi(t) - \hat{H}\psi(t)\|^2 \quad (12)$$

must be minimised for a given variational ansatz $\psi = \psi(\mathbf{z})$ with respect to the variational parameters \mathbf{z} . The variation of χ , while ψ is fixed, and the identification of χ with $\dot{\psi}$ leads to the necessary condition [27]

$$\mathbf{K}\dot{\mathbf{z}} = -i\mathbf{h}, \quad (13)$$

where the matrix \mathbf{K} and the vector \mathbf{h} are defined by

$$K_{ij} = \left\langle \frac{\partial \psi}{\partial z_i} \left| \frac{\partial \psi}{\partial z_j} \right. \right\rangle, \quad h_i = \left\langle \frac{\partial \psi}{\partial z_i} \left| \hat{H}\psi \right. \right\rangle. \quad (14)$$

The remaining task is to evaluate all integrals appearing in Eq. (14). Technical details are presented in Appendix A. Since the ground state in the GPE corresponds to a fixed

point of the equations of motion (13), we can find the ground state of a system by a nonlinear root search, for which we require

$$\dot{z}_i = \begin{cases} i\mu & \text{for } z_i \equiv \gamma^k, \\ 0 & \text{else,} \end{cases} \quad (15)$$

where μ is the chemical potential.

Stability and excitations in the framework of the TDVP are given by the linearised equations of motion, for which one first needs to rewrite the complex equations of motion (13) into real ones by defining the new vector of variational parameters $\tilde{\mathbf{z}}$ as $\tilde{\mathbf{z}} = (\text{Re } \mathbf{z}, \text{Im } \mathbf{z})$. The time-dependence of a small perturbation $\delta\tilde{\mathbf{z}}$ is then given by [2]

$$\delta\dot{\tilde{z}}_i = \sum_j \left. \frac{\partial \dot{\tilde{z}}_i}{\partial \tilde{z}_j} \right|_{\tilde{\mathbf{z}}=\tilde{\mathbf{z}}_0} \delta\tilde{z}_j \equiv \sum_j J_{ij} \delta\tilde{z}_j, \quad (16)$$

with the Jacobian \mathbf{J} evaluated at the fixed point $\tilde{\mathbf{z}}_0$. These linearised equations of motion are as usual solved by a harmonic time-dependence of the perturbation

$$\delta\tilde{\mathbf{z}}(t) = e^{i\omega t} \delta\tilde{\mathbf{z}}(0), \quad (17)$$

which leads to the eigenvalue problem

$$i\omega \delta\tilde{\mathbf{z}}(0) = \mathbf{J} \delta\tilde{\mathbf{z}}(0). \quad (18)$$

A real ω belongs to an oscillatory motion, as for real eigenvalues ω of the BDGE. The symmetry of the system, which leads to the quantum numbers m and π_z in the Bogoliubov spectrum, gives rise to a block structure of the Jacobian which is further explained in Appendix B.

The eigenvalues of the Jacobian and the BDGE can be directly compared. But is there also a relationship between the eigenvectors of the Jacobian $\delta\tilde{\mathbf{z}}$ and the eigenfunctions of the BDGE u and v ? For a given eigenvector $\delta\tilde{\mathbf{z}}$, a wave function can be constructed by taking the difference of the excitation with variational parameters $\tilde{\mathbf{z}}_0 + \delta\tilde{\mathbf{z}}$ and the wave function of the stationary solution with the parameters $\tilde{\mathbf{z}}_0$,

$$\delta\psi(\tilde{\mathbf{z}}_0, \delta\tilde{\mathbf{z}}) \equiv \psi(\tilde{\mathbf{z}}_0 + \delta\tilde{\mathbf{z}}) - \psi(\tilde{\mathbf{z}}_0). \quad (19)$$

Since we are dealing with an excitation in the linear regime, one can Taylor expand the first summand in Eq. (19) to first order in $\delta\tilde{\mathbf{z}}$. This yields the function [2]

$$\delta\psi = \delta\tilde{\mathbf{z}} \cdot \left. \frac{\partial \psi}{\partial \tilde{\mathbf{z}}} \right|_{\tilde{\mathbf{z}}=\tilde{\mathbf{z}}_0}, \quad (20)$$

which is the scalar product of the eigenvector and the gradient of the wave function with respect to the variational parameters evaluated at the stationary solution. Thus, every eigenvector $\delta\tilde{\mathbf{z}}$ belongs uniquely to a function $\delta\psi$.

As the Jacobian \mathbf{J} is real and a stable mode is represented by an imaginary eigenvalue $i\omega$, for every eigenvalue $i\omega$ with $\omega > 0$ there is also an eigenvalue $-i\omega$, therefore we can construct corresponding functions $\delta\psi_+$ and $\delta\psi_-$ which evolve in time as $\exp(i\omega t)$ and $\exp(-i\omega t)$, respectively. They can be combined to the perturbation

$$\delta\psi = \delta\psi_- e^{-i\omega t} + \delta\psi_+ e^{i\omega t}. \quad (21)$$

Comparing this with the Bogoliubov ansatz from Eq. (5) leads to the relationship

$$u \leftrightarrow \delta\psi_-, \quad v^* \leftrightarrow \delta\psi_+, \quad (22)$$

which links the eigenvectors of the Jacobian with the eigenfunctions of the BDGE.

2.3. Results for the BEC with scattering interaction

We now apply the variational ansatz (11) to a condensate with an attractive SRI. Fig. 3 shows the results, where $N_G = 5$ coupled Gaussians have been used (solid lines), compared to the full-numerical calculations (dotted lines). For the sake of clarity we distinguish between even modes in Fig. 3a and odd modes in Fig. 3b. One recognises that the lowest mode of each angular momentum and parity can perfectly be reproduced by the variational ansatz. Interestingly, as with our previous ansatz for spherically symmetric systems [4], the frequencies of the centre of mass oscillations (lowest odd $m = 0$ at $\omega = \sqrt{8}\omega_\rho$, lowest even $m = 1$ at $\omega = \omega_\rho$) agree, within numerical accuracy, with an arbitrary number of coupled Gaussians, even with $N_G = 1$. For the second lowest modes we also find a very good agreement as long as the scattering length is not close to the critical value. For the case $m = 0$, $\pi_z = 1$ even more eigenvalues of the Jacobian are close to the numerical results.

To demonstrate the power of our extended ansatz, we calculated eigenmodes for angular momenta up to $m = 6$ (see Fig. 4) for a fixed scattering length $Na/a_{\text{ho}} = -0.34$. Even for these angular momenta the lowest modes agree well. For the second excitations and lower angular momenta we find also a good agreement, however, the deviations of the variational and numerical results become larger for increasing angular momenta. Nevertheless, there is an obvious relationship between the eigenfrequencies of the Bogoliubov spectrum and the eigenvalues of the Jacobian, where our extended variational ansatz (11) – specific to cylindrically symmetric systems – has been used. Thus, the variational ansatz is a valid alternative to simulations on grids if one is interested only in the lowest modes.

2.4. Results for the dipolar BEC

We now want to include the DDI in the calculations and especially verify if the extended variational ansatz can describe the stability change for higher angular momenta $m > 0$. We first investigate the eigenmodes in the stable regime with a scattering length $Na/a_{\text{ho}} \geq 5$. Fig. 5 shows the comparison of both spectra for the angular momenta

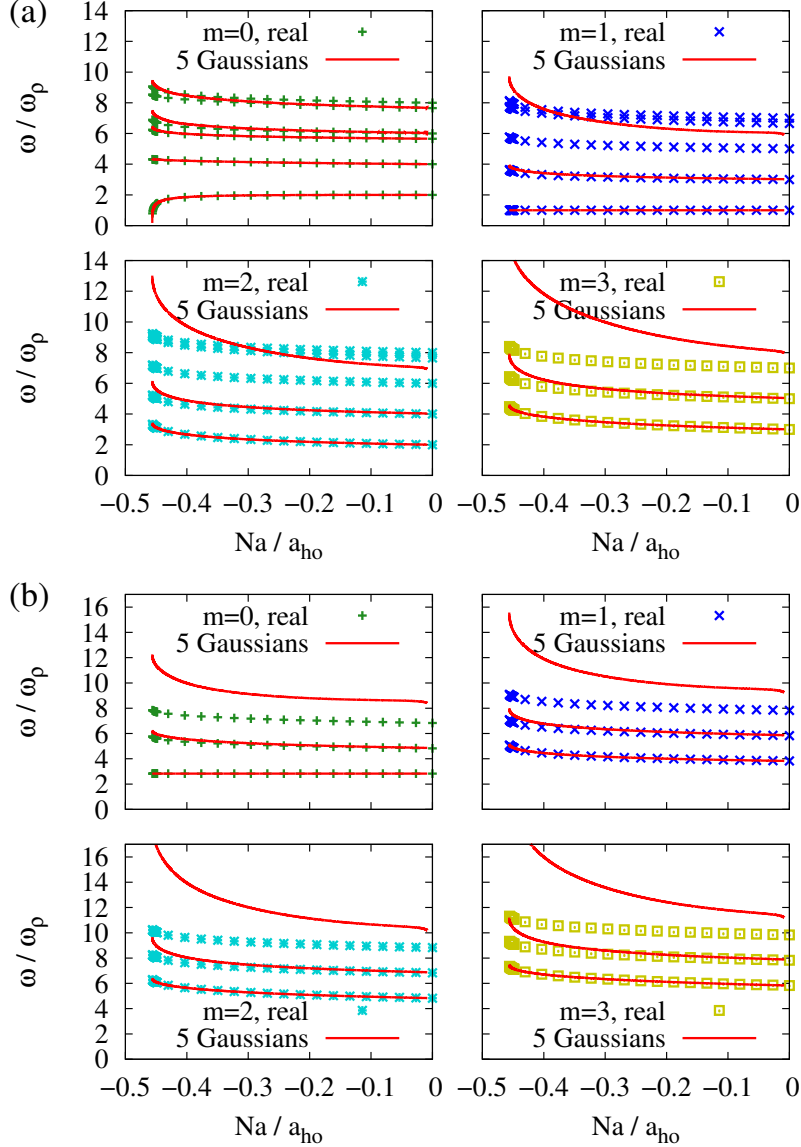


Figure 3. Comparison of the Bogoliubov spectrum for a BEC with SRI from Fig. 1a with the eigenvalues of the Jacobian obtained from the variational ansatz for even (a) and odd (b) parity. We find a very good agreement for the lowest two modes of each angular momentum and parity, only close to the critical scattering length deviations of the second lowest modes for $m > 0$ can be seen, which become larger for increasing angular momentum.

$m = 0, \dots, 3$. With 6 coupled Gaussians, the lowest modes of each angular momentum and parity (solid lines) are converged to their corresponding numerical frequencies (dotted lines). As in the case of the BEC without LRI, the centre of mass oscillations agree within numerical accuracy. For the modes with even parity, there is a good agreement even for the second lowest modes, where the differences become larger for rising scattering length and angular momentum. In the case of odd parity, the deviations for the second lowest modes become quite large for $m \geq 2$, when the scattering length

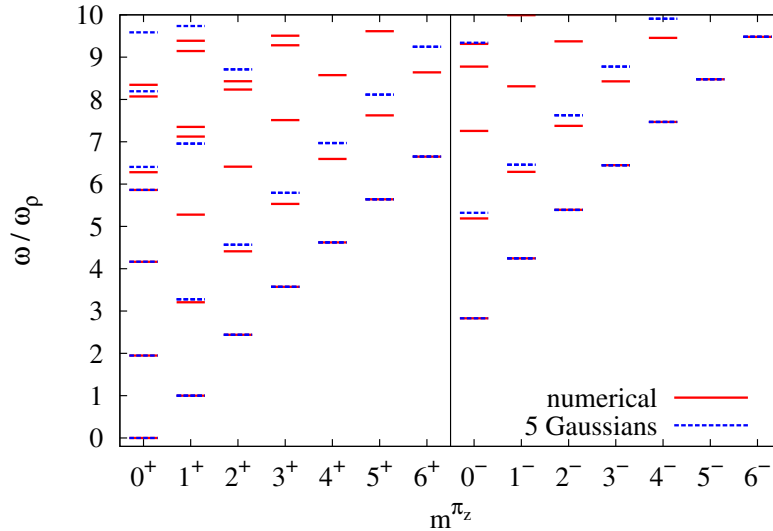


Figure 4. Comparison of both spectra as in Fig. 3, but here for a fixed scattering length of $Na/a_{\text{ho}} = -0.34$ and angular momenta up to $m = 6$. The variational ansatz also works for these modes and can describe the lowest modes of the Bogoliubov spectrum, therefore we are able to establish a connection between both methods.

is large.

We have also investigated eigenmodes with an angular momentum up to $m = 6$ in the stable regime. Fig. 6 shows the results for a fixed scattering length $Na/a_{\text{ho}} = 6$. The variational ansatz can reproduce the lowest modes even for these angular momenta and, since the scattering length is not too large, also the second lowest modes. For the case $m = 0$, $\pi_z = 1$, we find the lowest three modes converged, and a good agreement of the fourth lowest mode. These investigations show that the variational ansatz (11) can also reproduce the full-numerical Bogoliubov spectrum, if only the lowest modes are compared.

We now investigate the interesting case of a small negative scattering length, where the Bogoliubov spectrum shows unstable roton modes for different angular momenta (see Fig. 2). We focus here on the case $m = 3$, which cannot be described by the ansatz of coupled Gaussians Eq. (10), hence the extended variational ansatz is necessary. Fig. 7 shows the lowest modes with $m = 3$ obtained using different numbers of Gaussians (solid and dashed lines). For comparison the full-numerical results are also plotted (dotted line). We find that with an increasing number of coupled Gaussians the accuracy of the variational calculations increases gradually.

Other angular momenta show a similar behaviour, the convergence is in general better for lower angular momenta. Thus we can conclude, that the variational ansatz (11) can describe, though not quantitatively perfect, the dynamical instabilities of the Bogoliubov spectrum for angular momenta $m > 0$.

It is known that at the critical scattering length below which no stationary solution exists anymore an unstable collectively excited state emerges in a tangent bifurcation [3]

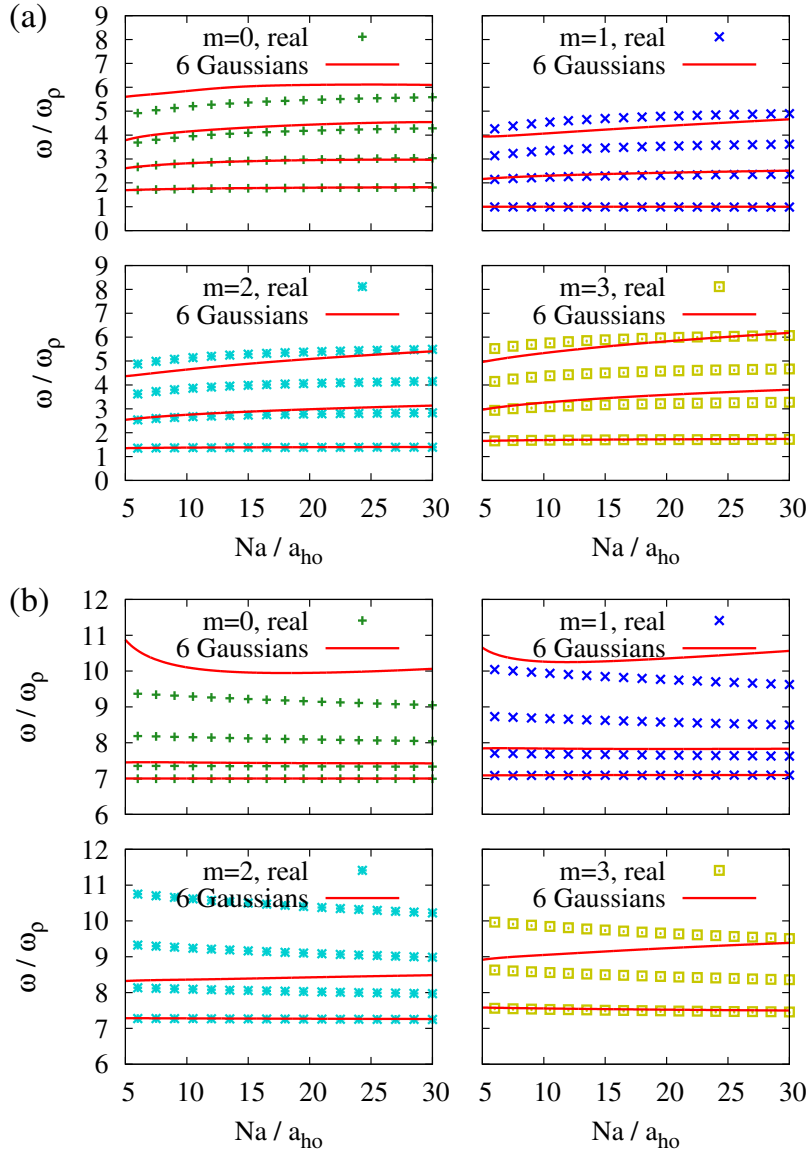


Figure 5. Comparison of the Bogoliubov spectrum for a dipolar BEC from Fig. 1b with the eigenvalues of the Jacobian obtained from the variational ansatz. Shown are the modes with even (a) and odd (b) parity in the stable regime with a scattering length $Na/a_{ho} \geq 5$. Whereas the two lowest modes agree well for even parity, for odd parity the second lowest modes differ quite clearly, especially for higher angular momenta $m \geq 2$.

in addition to the ground state (see the inset in Fig. 8). For condensates without DDI, this excited state is unstable with respect to an $m = 0$ excitation [3]. The variational approach offers the possibility to investigate this state of a dipolar BEC, which is not accessible to the full-numerical ITE method, and its collapse mechanism. Fig. 8 shows the imaginary frequencies of the excited state obtained with $N_G = 5$ Gaussians. As both states merge at the critical scattering length the same holds for the eigenfrequencies, and the excited state shares the instabilities of the ground state at the critical scattering

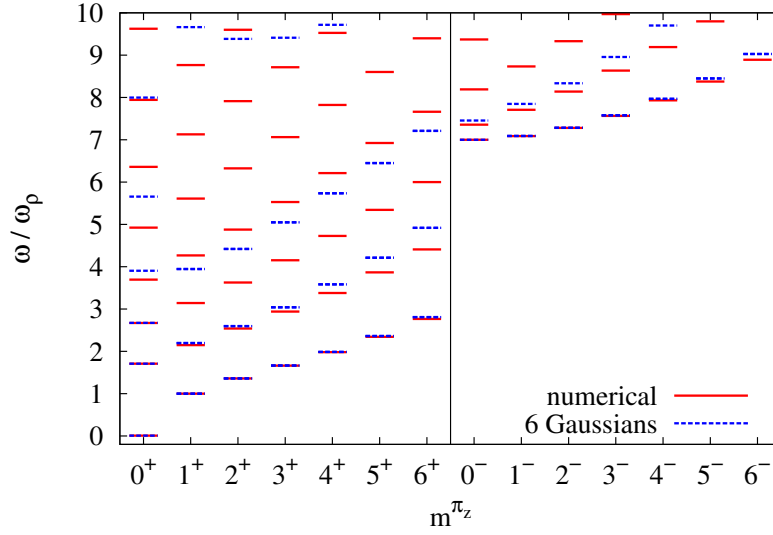


Figure 6. Comparison of both spectra as in Fig. 5, but here for a fixed scattering length of $Na/a_{ho} = 6$. For the lowest mode of each angular momentum and parity, there is a very good agreement. For the second lowest modes we find differences, which get larger for increasing angular momenta. The correspondence is slightly better for even than for odd modes. As in the case without LRI there is a link between the full-numerical Bogoliubov spectrum and the eigenvalues of the Jacobian resulting from the variational ansatz.

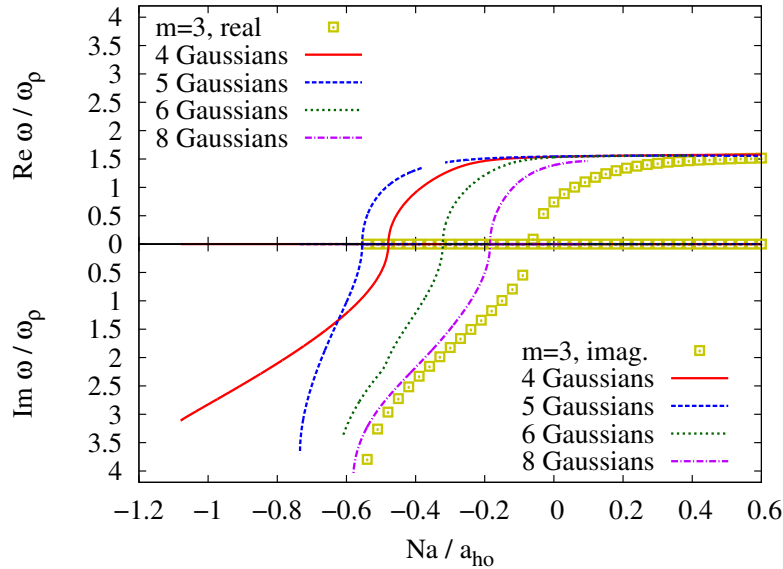


Figure 7. Lowest mode with $m = 3$ which turns unstable when the scattering length is decreased. Compared are the full-numerical frequencies (dotted line) with the results from the variational ansatz with different number of Gaussians (solid and dashed lines). The accuracy of the variational calculations increases gradually with the number of coupled Gaussians.

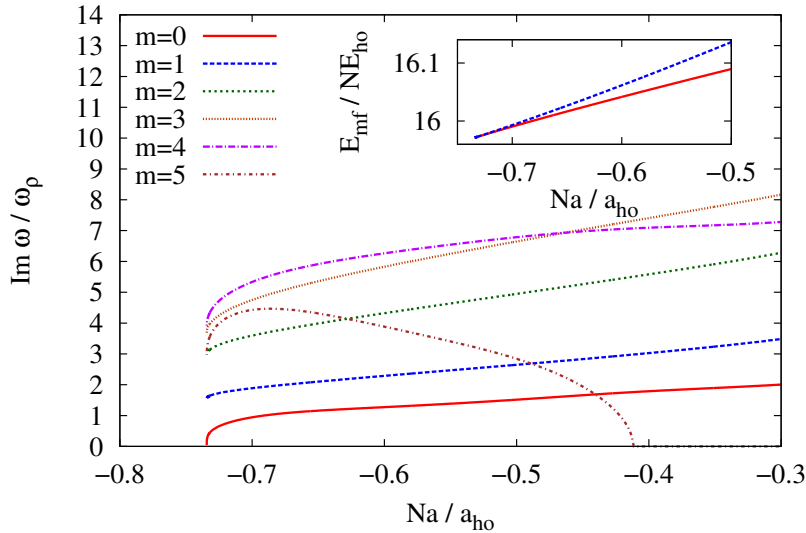


Figure 8. Imaginary frequencies of the excited state with $N_G = 5$ Gaussians. At the critical point the excited state shares the same instabilities as the ground state with additionally an $m = 0$ instability, which is typical for the collectively excited state. The inset shows the tangent bifurcation in the mean field energy $E_{\text{mf}}/NE_{\text{ho}}$ (N being the particle number) for the ground (solid) and excited (dashed) state, where $E_{\text{ho}} = \hbar\omega_\rho$ is the energy quantum of the harmonic oscillator.

length, except the additional $m = 0$ instability. In contrast to the case with SRI only or with monopolar LRI [4] the excited state of the dipolar BEC for the trapping frequencies is unlikely to collapse with $m = 0$ symmetry due to the additional instabilities for $m > 0$, which have a higher imaginary frequency and thus a larger collapse rate.

The $m = 5$ excitation in Fig. 8 changes its stability with increasing scattering length, in a similar way as the unstable modes of the ground state (see Fig. 7). Note, however, that this does not mean a global change of the stability due to the other unstable modes. The excited state stays unstable for all scattering lengths considered in our calculations.

2.5. Shape of Bogoliubov excitations

After linking the eigenvalues of the BDGE and the Jacobian of the time-dependent variational approach, we will check if there is also a direct correspondence between the eigenfunctions and eigenvectors of these two approaches. In Sec. 2.2 we discussed how to construct the functions $\delta\psi_-$ and $\delta\psi_+$ from the eigenvectors and how they are related to the functions u and v . For a better comparison of both methods, we use the usual normalisation of the Bogoliubov functions $\int d^3r [|u|^2 - |v|^2] = 1$ [1], and assume the same for the variational method, $\int d^3r [|\delta\psi_-|^2 - |\delta\psi_+|^2] = 1$. We point out that in calculating $\delta\psi_\pm$ there is no ambiguity, except for a global phase, which we choose in such a way that the functions are real. Fig. 9 shows the comparison of both methods

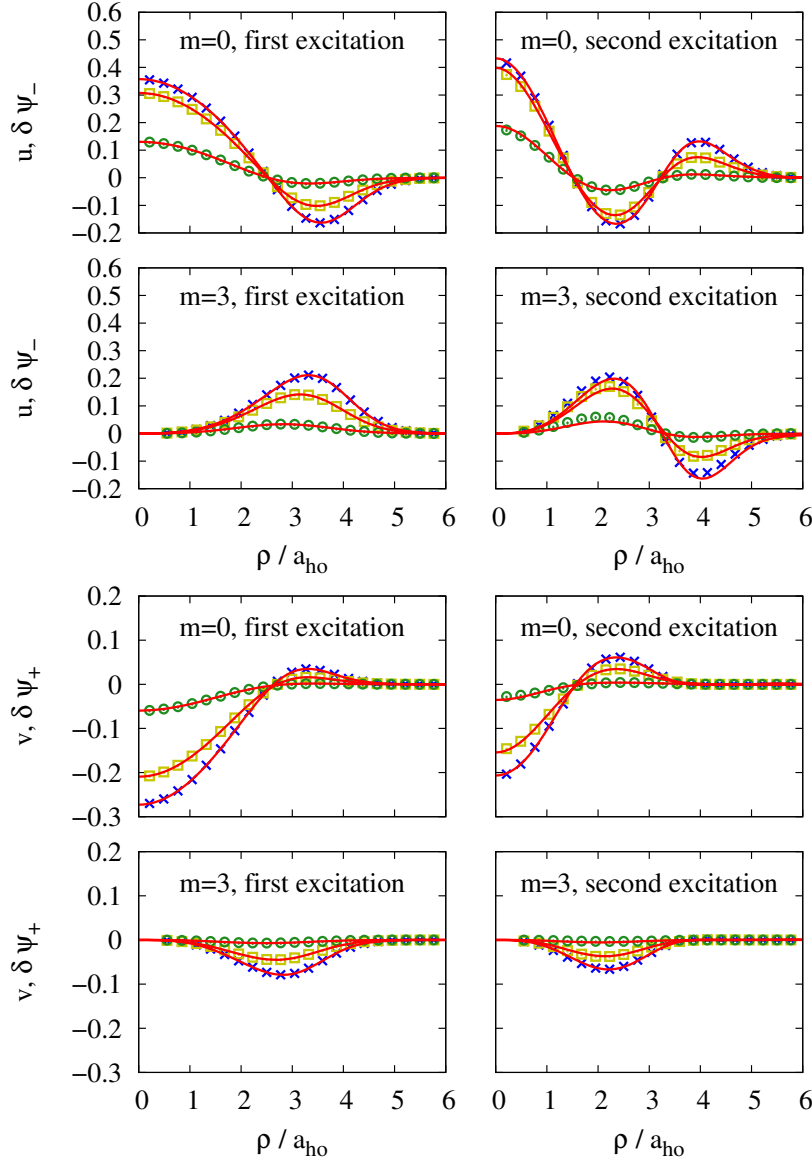


Figure 9. Radial dependence for the functions u , v and $\delta\psi_-$, $\delta\psi_+$ (red lines), respectively for different values of z [0 (blue crosses), $0.42a_{\text{ho}}$ (yellow squares), $0.84a_{\text{ho}}$ (green circles)], where $N_{\text{G}} = 8$ Gaussians have been used (see text for normalisation). Shown are the first two excitations for the angular momenta $m = 0, 3$ and a fixed scattering length of $Na/a_{\text{ho}} = 6$. All functions are chosen to be real. There is a very good agreement, only for the second $m = 3$ excitation there are small deviations.

for some modes. The first two functions u with $m = 0$ have one and two radial nodes, respectively, because the lowest mode with $m = 0$ represents the gauge mode, which is no physical excitation. For other angular momenta, the n -th excitation in ρ direction has $n - 1$ radial nodes. The asymptotic behaviour of all functions in Fig. 9 for $\rho \rightarrow 0$ is $\rho^{|m|}$. The nodal structure for the functions v is different. All v for $m = 0$ have one node, and for the other angular momenta zero nodes. For higher excitation numbers and angular momenta, the amplitude of v becomes smaller and smaller, indicating that

in these limits the coupling between u and v in the BDGE can be neglected, which is in accordance with previous calculations in the literature [1, 15, 28].

For the second excitation with $m = 3$ we find small deviations, which is to be expected, since there are also deviations in the eigenfrequencies (cf. Fig. 6). By comparing more eigenmodes we can conclude: The better the agreement of the eigenfunctions, the better is also the accordance of the frequencies. For higher modes, where there is no quantitative agreement between the eigenfrequencies, only the asymptotic behaviour and the nodal structure can be described by the variational ansatz, even though there is at least a qualitative agreement in those aspects.

The comparison of the eigenfunctions of the BDGE with those obtained from the eigenvectors of the Jacobian reveals a very good agreement. This is remarkable, since both functions originate from quite different approaches of stability. The extended variational ansatz (11) cannot only quantitatively describe the frequencies of the lowest modes, but also the shape of the oscillations, even for angular momenta, which were not accessible by the variational approach without the extension.

3. Dynamics

The extended variational ansatz (11) was proposed to find a direct relationship between the eigenvalues of the Jacobian and the eigenfrequencies of the BDGE. We have derived the equations of motion using the TDVP to calculate the Jacobian. The equations of motion (13) are not only valid in the vicinity of a fixed point, but for all variational parameters for which the integrals in the equations of motion converge. Wilson *et al* [9] simulated the dynamical evolution of a collapse for a dipolar condensate with biconcave structure by reducing the scattering length below the critical value, which yields a symmetry breaking collapse (*angular collapse*) with $m = 3$ symmetry. Rau *et al* [3] simulated this scenario within the variational framework with an ansatz of coupled Gaussians. However, as mentioned in Sec. 2.2, this ansatz cannot describe wave functions that exhibit the $m = 3$ symmetry. Motivated by these papers we will now integrate the equations of motion numerically with appropriate initial conditions to verify, whether or not the extended variational ansatz is also applicable in calculating the dynamics of dipolar condensates and especially to describe the angular collapse for arbitrary angular momenta, which is caused by the roton instability (cf. Secs. 2.1 and 2.4). To do so we only address the collapse of ground states with biconcave structure.

As a first example, we consider the system with $N_G = 4$ Gaussians and calculate the dynamics of an induced collapse by lowering the scattering length below the critical value. As an initial state for $t = 0$, we take the stable ground state for a scattering length of $Na/a_{ho} = 6$ and add a small perturbation for a specific angular momentum by changing the variational parameter $d_{m,p=0}^{k=1}$ to a small value larger than zero, e.g. $d_{m,p=0}^{k=1} = 2 \times 10^{-5}$, which is just a small perturbation of the ground state. We let the condensate evolve until $t\omega_\rho = 0.72$, after which the scattering length is linearly ramped down until $t\omega_\rho = 10.8$ to a value of $Na/a_{ho} = -0.6$, which is below the critical

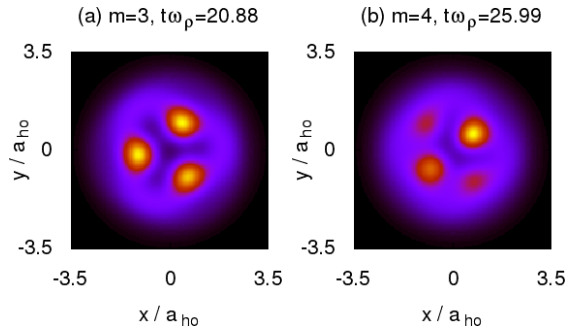


Figure 10. Modulus squared $|\psi|^2$ of the wave function of the collapsing dipolar condensate in a cut through the ($z = 0$)-plane. Bright (yellow) marks regions of high particle density, while dark (black) stands for low densities. For the calculations $N_G = 4$ Gaussians were used.

scattering length. The condensate then evolves at a fixed scattering length, until it collapses to a point, from where on no further integration is possible. We calculated this scenario for an initial $m = 3$ and $m = 4$ excitation, which cannot be described by the variational ansatz without the extension and thus is an advance as compared to previous calculations of a collapsing condensate within the variational framework [3].

Fig. 10 shows the resulting density of the collapsing condensate for both cases. For an initial $m = 3$ excitation, the collapsing cloud exhibits the clear shape with an $m = 3$ symmetry, the angular dependency is proportional to $\sin(3\phi)$. This result shows that the extended variational ansatz is not only able to describe the instability in the vicinity of the ground state, but also the nonlinear dynamics given by the equations of motion (13). If the initial state is perturbed by an $m = 4$ excitation, the resulting density distribution shows a superposition of several angular momenta. There are altogether four density peaks, of which two are significantly larger than the other two. The appearance of four peaks corresponds to an $m = 4$ symmetry, but the distribution of the particle density clearly belongs to $m = 2$. Of the two large peaks, one is slightly higher than the other one which indicates an $m = 1$ symmetry. The calculation shows that the different angular momenta do not evolve freely, but instead are coupled and influence each other. This is due to the nonlinearity of the GPE (1) which carries over to the equations of motion for the variational parameters.

There are many excitations one can add to the ground state as a perturbation. Above, we added specific eigenmodes to investigate the behaviour of the extended variational ansatz when considering the collapse dynamics. We now want to utilise a more physical motivated initial state. In Ref. [9] the authors added modes with weights determined by the Bose-Einstein distribution, which leads to

$$\psi_0(\rho, z) + \sum_{n,m} \sqrt{\frac{n_{n,m}}{N}} e^{2\pi i \alpha_{n,m}} [u_{n,m}(\rho, z) e^{im\phi} + v_{n,m}^*(\rho, z) e^{-im\phi}], \quad (23)$$

where ψ_0 is the ground state. The weight of each excitation, where m is the angular

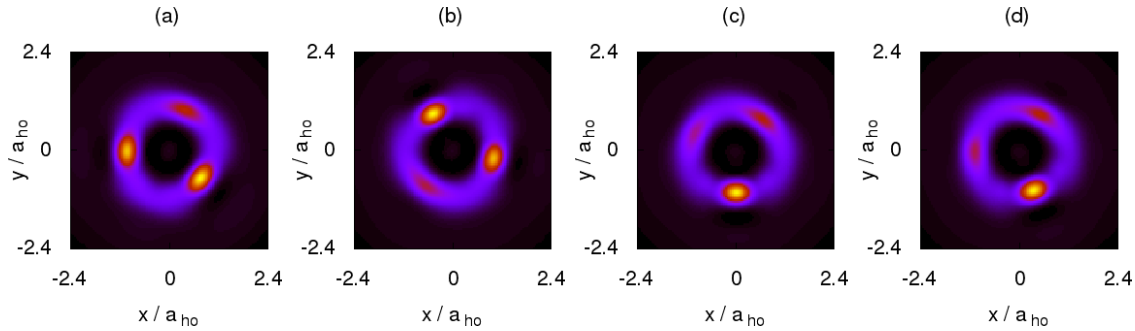


Figure 11. Particle densities of the collapsing cloud at $t\omega_\rho = 12.384$ with high (low) density represented by bright (dark) regions. All calculations were done with $N_G = 5$ Gaussians. The different random phases used to construct the initial state (see text) are the only differences in the four calculations. There are three density peaks each, but the overall rotation and the density distribution along the peaks are different.

momentum and n summarises the other quantum numbers, is given by

$$n_{n,m} = \left(e^{\hbar\omega_{n,m}/k_B T} - 1 \right)^{-1}. \quad (24)$$

Here, $\omega_{n,m}$ is the energy of each excitation, k_B the Boltzmann constant, and T the temperature. The quantities $\alpha_{n,m}$ in Eq. (23) determine the initial phase of each excitation and are random numbers between 0 and 1. The overall factor $1/\sqrt{N}$, with N the particle number, is necessary, since the wave function ψ is normalised to unity instead of N .

We now can make use of the relationship between the eigenvectors of the Jacobian and the eigenfunctions of the BDGE (Sec. 2.5) to prepare an initial state similar to that given by Eq. (23) within the variational framework, where instead of the functions, the eigenvectors of the variational parameters have to be added to the ground state vector. For the following calculations we simulate a condensate consisting of $N = 10000$ ^{52}Cr atoms at a temperature of $T = 100$ nK. We start with an initial wave function according to Eq. (23) and a scattering length of $Na/a_{\text{ho}} = 6$, which is ramped down to a value of $Na/a_{\text{ho}} = -3$ over a time of $\Delta t\omega_\rho = 14.68$.

We performed several calculations with this scenario, for which the only differences are the initial phases $\alpha_{n,m}$. As the scattering length decreases the particle density establishes its biconcave structure, which is a typical feature of dipolar BECs [6–9]. If the scattering length further decreases, the critical value is reached and the atomic cloud starts to collapse to the region with the highest density, which is on a ring around the centre. Due to the initial excitations with angular momentum $m > 0$, which are now unstable, the symmetry is broken and several density peaks emerge. Fig. 11 shows the density distribution of four different calculations shortly before collapse. Each condensate has three peaks located almost equidistantly on a ring. But the distribution along the ring differs: In Figs. 11 (a)-(b) there are two large peaks and a smaller one, while in Figs. 11 (c)-(d) it is the other way round. Additionally the initial phases determine the overall rotation of the collapsed condensate in the ($z = 0$)-plane. We can

conclude that both, the $m = 2$ and $m = 3$ mode, are responsible for the shape of the collapsed cloud, which corresponds to the numerical solution of the BDGE (see Fig. 2), in which both modes turn unstable almost simultaneously.

A question, which naturally arises, is how the number of Gaussians influences the dynamics calculation. We performed similar calculations with $N_G = 4$ and $N_G = 6$ Gaussians. With 4 Gaussians we find a different behaviour in that a collapse with $m = 2$ symmetry is favoured. However, with 6 Gaussians almost the same results as in the case with 5 Gaussians are obtained. The only difference is the time taken before the condensate collapses, which is shorter with 6 Gaussians. This can be explained by the fact that the critical scattering length is shifted to a higher value and thus the critical point is reached earlier during the simulation. The eigenfrequencies with our Gaussian ansatz do not fully agree with the full-numerical results (cf. Sec. 2.4), however, we expect the variational results to not being completely converged with 5 or 6 Gaussians.

4. Conclusion and outlook

We presented an extended variational ansatz, which is specific to cylindrically symmetric systems and which can describe arbitrary angular momenta, and derived the equations of motion for the variational parameters using the TDVP. The eigenfrequencies of two different systems (without and with DDI) were calculated using the variational ansatz and compared with the direct solutions of the BDGE. We found a good agreement of the lowest-lying modes and could confirm the direct relationship of both methods. This extended our investigations of spherically symmetric systems [4] and we could show that this agreement is of generic type, independent of the symmetry and the interactions.

The roton-instability of a pancake-shaped dipolar BEC was investigated using the extended ansatz. We could find instabilities for arbitrary values of the angular momenta, which is a great progress in comparison with the variational ansatz with coupled Gaussians without the extension. With more and more Gaussians we obtained gradually more accurate results within the variational framework. Thus, our variational method is a valid approximation to grid calculations.

We further constructed functions of the eigenvectors of the Jacobian and found that these functions agree very well with the solutions of the BDGE, as long as the corresponding eigenvalues agree. There is not only a direct link between the eigenfrequencies, but also between the eigenvectors and the eigenfunctions.

After considering the dynamics in the linear regime we directly integrated the nonlinear equations of motion and showed that our variational ansatz, assuming that the initial conditions and the scenario of the time-dependent scattering length are appropriately chosen, is capable of describing the angular collapse with arbitrary angular momenta. We used the relationship between the eigenvectors of the Jacobian and the eigenfunctions of the BDGE to construct an initial state which corresponds to a condensate in thermal equilibrium within the mean field approximation, and simulated a realistic experiment of the angular collapse. We found that the random initial phase

distribution strongly influences the shape of the collapsed atomic cloud, which makes the resulting shape of an experiment irreproducible.

Altogether it was shown that the extended variational ansatz is a significant progress compared to coupled Gaussians, and as yet unaccessible results could be obtained. Our ansatz is a valid alternative to calculate eigenfrequencies and shapes of elementary excitations, if the lowest eigenmodes of stable condensates are considered. The roton-instabilities can be obtained, but we could not find a good quantitative agreement, leaving our ansatz an approximation.

In future applications of the extended variational ansatz it would be possible to include the particle loss in the dynamics calculation, as the losses are necessary to accurately simulate a collapse scenario of a dipolar BEC [9,29]. Furthermore, our ansatz is applicable to dipolar BECs in a one-dimensional optical lattice [30–32] to calculate the ground state, stability, excitations and the dynamics. The direct relationship between the eigenvectors of the Jacobian and the eigenfunctions of the BDGE allows several applications of the variational approach, e. g. to describe a BEC at finite temperature, where a self-consistent solution of the GPE and BDGE is necessary [33].

Acknowledgments

This work was supported by Deutsche Forschungsgemeinschaft.

Appendix A. Calculation of the integrals for the variational ansatz

This appendix is dedicated to the integrals necessary for the matrix \mathbf{K} and the vector \mathbf{h} , which are defined by

$$K_{ij} = \left\langle \frac{\partial\psi}{\partial z_i} \middle| \frac{\partial\psi}{\partial z_j} \right\rangle = \int d^3r \left(\frac{\partial\psi}{\partial z_i}(\mathbf{r}) \right)^* \frac{\partial\psi}{\partial z_j}(\mathbf{r}), \quad (\text{A.1a})$$

$$h_i = \left\langle \frac{\partial\psi}{\partial z_i} \middle| \hat{H}\psi \right\rangle = \int d^3r \left(\frac{\partial\psi}{\partial z_i}(\mathbf{r}) \right)^* \hat{H}\psi(\mathbf{r}), \quad (\text{A.1b})$$

to set up the equations of motion (13) of the variational ansatz (11) via the time-dependent variational principle. We write the variational ansatz in the form

$$\psi = \sum_{k=1}^{N_G} \sum_m \sum_{p=0,1} d_{m,p}^k \rho^{|m|} z^p e^{im\phi} e^{-A_\rho^k \rho^2 - A_z^k z^2 - p_z^k z - \gamma^k}, \quad (\text{A.2})$$

where $d_{0,0}^k \equiv 1$ and $d_{0,1}^k \equiv 0$ are no variational parameters, but constants. We further introduce the abbreviations

$$\langle z_i | z_j \rangle \equiv \left\langle \frac{\partial\psi}{\partial z_i} \middle| \frac{\partial\psi}{\partial z_j} \right\rangle, \quad \langle z_i | X\psi \rangle \equiv \left\langle \frac{\partial\psi}{\partial z_i} \middle| X\psi \right\rangle \quad (\text{A.3})$$

for the matrix elements, where X is an operator of the mean field Hamiltonian $H = T + V_{\text{ext}} + \Phi_s + \Phi_d$ with the kinetic part, the external potential and the scattering and dipolar mean field potentials.

We do not give a detailed way on how to calculate all necessary integrals, nor do we present all results. We rather want to sketch the calculations and give results of some examples. For all details we refer to the master thesis of one of the authors [34].

Appendix A.1. Integrals of the K-matrix

Before giving the results, we define the abbreviations

$$A_\rho^{kl} \equiv A_\rho^k + (A_\rho^l)^*, \quad A_z^{kl} \equiv A_z^k + (A_z^l)^*, \quad p_z^{kl} \equiv p_z^k + (p_z^l)^*, \quad \gamma^{kl} \equiv \gamma^k + (\gamma^l)^* \quad (\text{A.4})$$

and the basic integrals

$$I^{kl}(m, n) \equiv \int_0^\infty d\rho \rho^{2m-1} e^{-A_\rho^{kl} \rho^2} \int_{-\infty}^\infty dz z^n e^{-A_z^{kl} z^2 - p_z^{kl} z} e^{-\gamma^{kl}} = e^{-\gamma^{kl}} \frac{\Gamma(m)}{2(A_\rho^{kl})^m} I_z^{kl}(n). \quad (\text{A.5})$$

The ρ integral can be identified with the gamma function by a simple substitution. The z integral is a Gaussian integral for $n = 0$, higher orders can be obtained by the recursion formula

$$I_z^{kl}(n+1) = -\frac{\partial}{\partial p_z^{kl}} I_z^{kl}(n). \quad (\text{A.6})$$

The integrals of the matrix \mathbf{K} then yield

$$\langle d_{m_2, p_2}^l | d_{m_1, p_1}^k \rangle = 2\pi \delta_{m_1 m_2} I^{kl}(|m_1| + 1, p_1 + p_2), \quad (\text{A.7a})$$

$$\langle d_{m_2, p_2}^l | A_\rho^k \rangle = -2\pi \sum_{p_1} I^{kl}(|m_2| + 2, p_1 + p_2), \quad (\text{A.7b})$$

$$\langle d_{m_2, p_2}^l | A_z^k \rangle = -2\pi \sum_{p_1} I^{kl}(|m_2| + 1, p_1 + p_2 + 2), \quad (\text{A.7c})$$

$$\langle d_{m_2, p_2}^l | p_z^k \rangle = -2\pi \sum_{p_1} I^{kl}(|m_2| + 1, p_1 + p_2 + 1), \quad (\text{A.7d})$$

$$\langle d_{m_2, p_2}^l | \gamma^k \rangle = -2\pi \sum_{p_1} I^{kl}(|m_2| + 1, p_1 + p_2). \quad (\text{A.7e})$$

The other integrals can similarly be expressed by Eq. (A.5).

Appendix A.2. Integrals of the kinetic term

For the integrals of the kinetic term the action of the Laplacian on the variational ansatz is necessary. This is most easily evaluated in cylindrical coordinates. The integrals can then be expressed by Eq. (A.5). For the d parameters, e. g., one obtains

$$\begin{aligned} \langle d_{m_2, p_2}^l | T\psi \rangle / \hbar\omega_\rho &= \pi \sum_k \sum_{p_1} d_{m_2, p_1}^k \left\{ [4(|m_2| + 1)A_\rho^k + 2(2p_1 + 1)A_z^k - (p_z^k)^2] \right. \\ &\times I^{kl}(|m_2| + 1, p_1 + p_2) + [2p_1 p_z^k] I^{kl}(|m_2| + 2, p_2) - [4p_z^k A_z^k] I^{kl}(|m_2| + 2, p_1 + p_2 + 1) \\ &\left. - [4(A_z^k)^2] I^{kl}(|m_2| + 2, p_1 + p_2 + 2) - [4(A_\rho^k)^2] I^{kl}(|m_2| + 3, p_1 + p_2) \right\}. \quad (\text{A.8}) \end{aligned}$$

Appendix A.3. Integrals of the trapping potential

The trapping potential is of the form $V_{\text{ext}}/\hbar\omega_\rho = \frac{M}{2}\omega_\rho^2(\rho^2 + \lambda^2 z^2)$. Thus, the corresponding integrals are easy to evaluate. As an example we obtain

$$\begin{aligned} \langle d_{m_2, p_2}^l | V_{\text{ext}} \psi \rangle / \hbar\omega_\rho &= \pi \sum_k \sum_{p_1} d_{m_2, p_1}^k \\ &\times \left(I^{kl}(|m_2| + 2, p_1 + p_2) + \lambda^2 I^{kl}(|m_2| + 1, p_1 + p_2 + 2) \right). \end{aligned} \quad (\text{A.9})$$

Appendix A.4. Integrals of the scattering interaction

The integrals for the interaction terms require some more attention. First an expression for the modulus squared wave function $|\psi|^2$ is needed. This enters the integrals for the interaction potentials. The scattering interaction is easier to calculate, since this kind of interaction is local, in contrast to the DDI.

We further need new abbreviations, which depend on four indices and which are defined by

$$A_\rho^{ijkl} \equiv A_\rho^{ij} + A_\rho^{kl}, \quad A_z^{ijkl} \equiv A_z^{ij} + A_z^{kl}, \quad p_z^{ijkl} \equiv p_z^{ij} + p_z^{kl}, \quad \gamma^{ijkl} \equiv \gamma^{ij} + \gamma^{kl}. \quad (\text{A.10})$$

The new basic integral, $I^{ijkl}(m, n)$, can be obtained from the former one, Eq. (A.5), by substituting all indices kl with $ijkl$. The scattering integral then reads

$$\begin{aligned} \langle d_{m_2, p_2}^l | \Phi_s \psi \rangle / \hbar\omega_\rho &= 8\pi^2 \frac{Na}{a_{\text{ho}}} \sum_{i, j, k} \sum_{m_1, m_3, m_4} \sum_{p_1, p_3, p_4} (d_{m_4, p_4}^j)^* d_{m_3, p_3}^i d_{m_1, p_1}^k \delta_{m_1 + m_3, m_2 + m_4} \\ &\times I^{ijkl} \left(\frac{|m_1| + |m_2| + |m_3| + |m_4| + 2}{2}, p_1 + p_2 + p_3 + p_4 \right). \end{aligned} \quad (\text{A.11})$$

Appendix A.5. Integrals of the dipolar interaction

In order to calculate the integrals of the dipolar interaction, we first need the expression for the mean field potential Φ_d . This potential can be rewritten using Fourier transforms and the convolution theorem, which yields [35]

$$\Phi_d(\mathbf{r}) = \mathcal{F}^{-1}[\tilde{V}_d(\mathbf{k}) \cdot \tilde{n}(\mathbf{k})], \quad (\text{A.12})$$

where the functions with tilde designate the Fourier transforms of the dipole potential and the particle density. The transform of the dipole potential is well-known to be [35]

$$\tilde{V}_d(\mathbf{k}) / \hbar\omega_\rho = \frac{4\pi}{3} \left(3 \frac{k_z^2}{k^2} - 1 \right) D/N. \quad (\text{A.13})$$

Our next task is to calculate $\tilde{n}(\mathbf{k})$. Writing the square of the absolute value of the wave function with the given variational ansatz, one notices that the angular dependency is of the form $\exp(im\phi)$ with some $m \in \mathbb{Z}$. In [15] it was noted that the three-dimensional Fourier transform of such a function can be expressed as a one-dimensional Hankel

transform for the ρ direction and a remaining one-dimensional Fourier transform in the z direction. The Hankel transform brings in the Bessel function, and the integral can be worked out by Taylor expanding the Bessel function. The Fourier transform is a Gaussian integral with linear terms and variable powers of z , for which an analytical expression can be found in established tables of integrals [36, Eq. 3.462.2].

In the original integral, $\langle d|\Phi_d\psi\rangle$, the integral over \mathbf{r} is similar to the Fourier transform of $|\psi|^2$ and can easily be expressed in the same way, which yields the intermediate result

$$\begin{aligned} \langle d_{m_2, p_2}^l | \Phi_d \psi \rangle &= \frac{1}{2\pi} \sum_{i,j,k} \sum_{m_1, m_3, m_4} \sum_{p_1, p_3, p_4} e^{-\gamma^{ijkl}} (d_{m_4, p_4}^j)^* d_{m_3, p_3}^i d_{m_1, p_1}^k \sigma_{m_1-m_2} \sigma_{m_3-m_4} \\ &\times \frac{i^{m_1-m_2-m_3+m_4}}{2^{|m_1-m_2|+|m_3-m_4|+2}} (A_\rho^{kl})^{-|m_1-m_2|-\mu_{m_1, m_2}-1} (A_\rho^{ij})^{-|m_3-m_4|-\mu_{m_3, m_4}-1} \\ &\times \sum_{\alpha=0}^{\mu_{m_1, m_2}} \sum_{\beta=0}^{\mu_{m_3, m_4}} \binom{\mu_{m_1, m_2}}{\alpha} \binom{\mu_{m_3, m_4}}{\beta} (4A_\rho^{kl})^\alpha (4A_\rho^{ij})^\beta (-1)^{\mu_{m_1, m_2}+\mu_{m_3, m_4}} \\ &\times (-|m_1-m_2|-\mu_{m_1, m_2})_{\mu_{m_1, m_2}-\alpha} (-|m_3-m_4|-\mu_{m_3, m_4})_{\mu_{m_3, m_4}-\beta} \times I_k, \end{aligned} \quad (\text{A.14})$$

where we defined

$$\sigma_m \equiv (\text{sign } m)^m, \quad \mu_{m_1, m_2} \equiv \begin{cases} 0 & \text{for sign } m_1 \neq \text{sign } m_2, \\ \min(|m_1|, |m_2|) & \text{otherwise,} \end{cases} \quad (\text{A.15})$$

and used the Pochhammer symbol $(a)_n$, which is defined by

$$(a)_n \equiv a(a-1)(a-2)\cdots(a-n+1) = \frac{\Gamma(a+1)}{\Gamma(a-n+1)}. \quad (\text{A.16})$$

The remaining three dimensional integral I_k reads

$$\begin{aligned} I_k &= \int d^3k e^{i(m_1+m_3-m_2-m_3)k_\phi} e^{-k_\rho^2/4A_\rho^{ij}} e^{-k_\rho^2/4A_\rho^{kl}} \\ &\times k_\rho^{2(\alpha+\beta)+|m_1-m_2|+|m_3-m_4|} \tilde{I}_{-z}^{kl}(p_1+p_2) \tilde{I}_z^{ij}(p_3+p_4) \tilde{V}_d(\mathbf{k}), \end{aligned} \quad (\text{A.17})$$

with the z integrals

$$\tilde{I}_z^{ij}(p) \equiv \int_{-\infty}^{\infty} dz z^p e^{-A_z^{ij} z^2 - (p_z^{ij} + ik_z)z}, \quad (\text{A.18a})$$

$$\tilde{I}_{-z}^{kl}(p) \equiv \int_{-\infty}^{\infty} dz z^p e^{-A_z^{kl} z^2 - (p_z^{kl} - ik_z)z}, \quad (\text{A.18b})$$

which are evaluated in Ref. [36, Eq. 3.462.2]. The Fourier transform of the dipole potential consists of two parts, $V_d = (4\pi k_z^2/k^2 - 4\pi/3)\hbar\omega_\rho D/N \equiv V_d^1 + V_d^2$. The integral

of I_k containing V_d^2 is equivalent to the integrals of the scattering interaction \S , and requires no further attention. The part of I_k with V_d^1 , which we denote by I_k^1 , can be rewritten to

$$I_k^1/\hbar\omega_\rho = 4\pi^2(D/N)\delta_{m_1+m_3,m_2+m_4}n!(\alpha_\rho^{ijkl})^n \times \int_1^\infty dt t^{-(n+1)} \int_{-\infty}^\infty dk_z k_z^2 e^{-(t-1)\alpha_\rho^{ijkl}k_z^2} \tilde{I}_{-z}^{kl}(p_1+p_2)\tilde{I}_z^{ij}(p_3+p_4). \quad (\text{A.19})$$

The k_z integral is of Gaussian type, and similar to \tilde{I}_{-z}^{kl} and \tilde{I}_z^{ij} . The remaining t integral can be expressed by the hypergeometric Function ${}_2F_1$ [37], assuming all parameters p_z^k are zero. In the general case, the t integral can be efficiently evaluated using a Taylor series.

Appendix B. Structure of the Jacobian

The solutions of the BDGE (6) can be classified by the quantum numbers m and π_z , which express the symmetries of the system. Applying the TDVP and linearizing the equations of motion yields an alternative description of linear oscillations and stability, in which the Jacobian \mathbf{J} plays a central role. The Jacobian, similar to the BDGE, also express the symmetries of the system and the quantum numbers, in that it assumes a block structure, which can in general be written as

$$\mathbf{J} = \left(\left\{ \mathbf{J}_{\pm m}^{\pi_z} \right\} \right) = \begin{pmatrix} \mathbf{J}_0^{+1} & & & \\ & \mathbf{J}_0^{-1} & & \\ & & \mathbf{J}_{\pm 1}^{+1} & \\ & & & \mathbf{J}_{\pm 1}^{-1} \\ & & & & \ddots \end{pmatrix}, \quad (\text{B.1})$$

where $\mathbf{J}_{\pm m}^{\pi_z}$ is the submatrix belonging to the angular momenta $\pm m$ and the parity π_z . This block structure allows one to set up and diagonalise the Jacobian for each m and π_z individually, analogously to solving the BDGE. The only difference is that in the Jacobian the angular momenta m and $-m$ are coupled, which is due to the coupling of those angular momenta in the integrals necessary for the equations of motion (cf. Appendix A).

A simple example, which shows that the coupling may not be neglected, is the submatrix of the $m = \pm 1$, $\pi_z = 1$ Jacobian obtained with $N_G = 1$ Gaussian, for a dipolar BEC with $\lambda = 7$ and $D = 30$

$$\mathbf{J}_{\pm 1}^{+1} = \begin{pmatrix} 0 & -2.5936 & 0 & -2.3931 \\ 2.5936 & 0 & -2.3931 & 0 \\ 0 & -2.3931 & 0 & -2.5936 \\ -2.3931 & 0 & 2.5936 & 0 \end{pmatrix} \omega_\rho, \quad (\text{B.2})$$

\S The Fourier transform of $V_s = 4\pi Na/a_{\text{ho}}\delta(\mathbf{r})$ is $4\pi Na/a_{\text{ho}}$, and thus proportional to V_d^2 . This means that the whole integral of this part is equivalent to the integrals of the scattering interaction.

where the variational parameters are ordered as $\tilde{z} = (\text{Re } d_{1,0}^0, \text{Im } d_{1,0}^0, \text{Re } d_{-1,0}^0, \text{Im } d_{-1,0}^0)$ for a scattering length of $Na/a_{\text{ho}} = 6$. The eigenvalues of the matrix (B.2) are $(+i\omega_\rho, +i\omega_\rho, -i\omega_\rho, -i\omega_\rho)$. The eigenvectors of the eigenvalue $+i\omega_\rho$ can then be combined to an eigenvector belonging to $m = 1$ and another eigenvector for $m = -1$, the same holds for the eigenvalue $-i\omega_\rho$. In general, for arbitrary number of Gaussians and angular momenta, by taking appropriate linear combinations of the eigenvectors, eigenvectors belonging to a specific angular momentum $+m$ or $-m$ can be obtained.

References

- [1] L. P. Pitaevskii and S. Stringari. *Bose-Einstein Condensation*. Oxford University Press, 2003.
- [2] S. Rau, J. Main, and G. Wunner. Variational methods with coupled Gaussian functions for Bose-Einstein condensates with long-range interactions. I. General concept. *Phys. Rev. A*, 82:023610, 2010.
- [3] S. Rau, J. Main, H. Cartarius, P. Köberle, and G. Wunner. Variational methods with coupled Gaussian functions for Bose-Einstein condensates with long-range interactions. II. Applications. *Phys. Rev. A*, 82:023611, 2010.
- [4] M. Kreibich, J. Main, and G. Wunner. Relation between the eigenfrequencies of Bogoliubov excitations of Bose-Einstein condensates and the eigenvalues of the Jacobian in a time-dependent variational approach. *Phys. Rev. A*, 86:013608, 2012.
- [5] V. M. Pérez-García, H. Michinel, J. I. Cirac, M. Lewenstein, and P. Zoller. Dynamics of Bose-Einstein condensates: Variational solutions of the Gross-Pitaevskii equations. *Phys. Rev. A*, 56:1424–1432, 1997.
- [6] S. Ronen, D. C. E. Bortolotti, and J. L. Bohn. Radial and Angular Rotons in Trapped Dipolar Gases. *Phys. Rev. Lett.*, 98:030406, 2007.
- [7] O. Dutta and P. Meystre. Ground-state structure and stability of dipolar condensates in anisotropic traps. *Phys. Rev. A*, 75:053604, 2007.
- [8] S. Rau, J. Main, P. Köberle, and G. Wunner. Pitchfork bifurcations in blood-cell-shaped dipolar Bose-Einstein condensates. *Phys. Rev. A*, 81:031605(R), 2010.
- [9] R. M. Wilson, S. Ronen, and J. L. Bohn. Angular collapse of dipolar Bose-Einstein condensates. *Phys. Rev. A*, 80:023614, 2009.
- [10] D. Buccoliero, A. S. Desyatnikov, W. Krolikowski, and Y. S. Kivshar. Laguerre and Hermite Soliton Clusters in Nonlocal Nonlinear Media. *Phys. Rev. Lett.*, 98:053901, 2007.
- [11] D. Buccoliero and A. S. Desyatnikov. Quasi-periodic transformations of nonlocal spatial solitons. *Opt. Express*, 17:9608–9613, 2009.
- [12] F. Maucher, S. Skupin, M. Shen, and W. Krolikowski. Rotating three-dimensional solitons in Bose-Einstein condensates with gravitylike attractive nonlocal interaction. *Phys. Rev. A*, 81:063617, 2010.
- [13] J. Stuhler, A. Griesmaier, T. Koch, M. Fattori, T. Pfau, S. Giovanazzi, P. Pedri, and L. Santos. Observation of Dipole-Dipole Interaction in a Degenerate Quantum Gas. *Phys. Rev. Lett.*, 95:150406, 2005.
- [14] A. Griesmaier, J. Werner, S. Hensler, J. Stuhler, and T. Pfau. Bose-Einstein Condensation of Chromium. *Phys. Rev. Lett.*, 94:160401, 2005.
- [15] S. Ronen, D. C. E. Bortolotti, and J. L. Bohn. Bogoliubov modes of a dipolar condensate in a cylindrical trap. *Phys. Rev. A*, 74:013623, 2006.
- [16] D. S. Jin, J. R. Ensher, M. R. Matthews, C. E. Wieman, and E. A. Cornell. Collective Excitations of a Bose-Einstein Condensate in a Dilute Gas. *Phys. Rev. Lett.*, 77:420–423, 1996.
- [17] S. Inouye, M. R. Andrews, J. Stenger, H.-J. Miesner, D. M. Stamper-Kurn, and W. Ketterle. Observation of Feshbach resonances in a Bose-Einstein condensate. *Nature*, 392:151–154, 1998.

- [18] M. D. Feit, J. A. Fleck Jr., and A. Steiger. Solution of the Schrödinger equation by a spectral method. *J. Comput. Phys.*, 47:412–433, 1982.
- [19] W. E. Arnoldi. The principle of minimized iterations in the solution of the matrix eigenvalue problem. *Q. Appl. Math.*, 9:17–29, 1951.
- [20] R. B. Lehoucq, D. C. Sorensen, and C. Yang. ARPACK USERS GUIDE: Solution of Large Scale Eigenvalue Problems by Implicitly Restarted Arnoldi Methods, 1997.
- [21] J. L. Roberts, N. R. Claussen, S. L. Cornish, E. A. Donley, E. A. Cornell, and C. E. Wieman. Controlled Collapse of a Bose-Einstein Condensate. *Phys. Rev. Lett.*, 86:4211–4214, 2001.
- [22] A. Gammal, T. Frederico, and L. Tomio. Critical number of atoms for attractive Bose-Einstein condensates with cylindrically symmetrical traps. *Phys. Rev. A*, 64:055602, 2001.
- [23] T. Koch, T. Lahaye, J. Metz, B. Fröhlich, A. Griesmaier, and T. Pfau. Stabilization of a purely dipolar quantum gas against collapse. *Nat. Phys.*, 5:218–222, 2008.
- [24] M. Edwards, P. A. Ruprecht, K. Burnett, R. J. Dodd, and C. W. Clark. Collective Excitations of Atomic Bose-Einstein Condensates. *Phys. Rev. Lett.*, 77:1671–1674, 1996.
- [25] A. D. McLachlan. A variational solution of the time-dependent Schrodinger equation. *Mol. Phys.*, 8:39–44, 1964.
- [26] P. A. M. Dirac. Note on Exchange Phenomena in the Thomas Atom. *Math. Proc. Cambridge*, 26:376–385, 1930.
- [27] H. Cartarius, T. Fabčić, J. Main, and G. Wunner. Dynamics and stability of Bose-Einstein condensates with attractive $1/r$ interaction. *Phys. Rev. A*, 78:013615, 2008.
- [28] F. Dalfovo, S. Giorgini, M. Guilleumas, L. Pitaevskii, and S. Stringari. Collective and single-particle excitations of a trapped Bose gas. *Phys. Rev. A*, 56:3840–3845, 1997.
- [29] T. Lahaye, J. Metz, B. Fröhlich, T. Koch, M. Meister, A. Griesmaier, T. Pfau, H. Saito, Y. Kawaguchi, and M. Ueda. d -Wave Collapse and Explosion of a Dipolar Bose-Einstein Condensate. *Phys. Rev. Lett.*, 101:080401, 2008.
- [30] P. Köberle and G. Wunner. Phonon instability and self-organized structures in multilayer stacks of confined dipolar Bose-Einstein condensates in optical lattices. *Phys. Rev. A*, 80:063601, 2009.
- [31] A. Junginger, J. Main, and G. Wunner. Variational calculations on multilayer stacks of dipolar Bose-Einstein condensates. *Phys. Rev. A*, 82:023602, 2010.
- [32] R. M. Wilson and J. L. Bohn. Emergent structure in a dipolar Bose gas in a one-dimensional lattice. *Phys. Rev. A*, 83:023623, 2011.
- [33] N. P. Proukakis and B. Jackson. Finite-temperature models of Bose-Einstein condensation. *J. Phys. B*, 41:203002, 2008.
- [34] M. Kreibich. Diploma thesis, Universität Stuttgart, 2011, available at http://itp1.uni-stuttgart.de/publikationen/abschlussarbeiten/kreibich_diplom_2011.pdf.
- [35] K. Góral and L. Santos. Ground state and elementary excitations of single and binary Bose-Einstein condensates of trapped dipolar gases. *Phys. Rev. A*, 66:023613, 2002.
- [36] I. S. Gradshteyn and I. M. Ryzhik. *Table of Integrals, Series, and Products*. Academic Press, New York and London, 4th edition, 1965.
- [37] M. Abramowitz and I. A. Stegun. *Handbook of Mathematical Functions*. United States Department of Commerce, 10th edition, 1972.